Dielectric Studies of Poly(ethylene oxide)/ Poly(styrene-*co*-*p*-hydroxystyrene) Blends: Influence of Hydrogen Bonding on the Dynamics of Amorphous Blends

Xing Jin, Shihai Zhang, and James Runt*

Department of Materials Science and Engineering, and Materials Research Institute, The Pennsylvania State University, University Park, Pennsylvania 16802

Received June 26, 2003; Revised Manuscript Received August 1, 2003

ABSTRACT: The segmental dynamics of a poly(styrene-*co*-*p*-hydroxystyrene) random copolymer [SHS, 50 wt % HS] and its amorphous, melt-miscible blends with poly(ethylene oxide) were investigated using broadband dielectric relaxation spectroscopy. The fragility of the neat copolymer was found to be close to that of polystyrene with comparable molecular weight, consistent with the idea that intramolecular hydrogen bonding primarily enhances the monomer friction coefficient and T_g, while having little effect on fragility. Despite the large mobility difference between the component polymers, a single cooperative segmental relaxation is observed for the blends (SHS concentration ≥ 60%), demonstrating the coupling ability of intermolecular hydrogen bonds. Blend fragility increased significantly with SHS content, reflecting the combined contribution of the two components. The most intriguing finding was a fast process in blends containing ≥80 wt % SHS. The available evidence supports its assignment to noncooperative segmental relaxation of PEO repeat units, having some similarities to the modified segmental dynamics of nanoconfined polymers.

1. Introduction

It has been widely reported that the relaxation times and temperature dependences of individual components are significantly different in many globally miscible polymer blends and disordered diblock copolymers.[1] This phenomenon is attributed to nanoscale heterogeneities and can be detected by nuclear magnetic resonance (NMR), dielectric relaxation spectroscopy (DRS), and dynamic mechanical analysis (DMA) but not differential scanning calorimetry (DSC), since the latter can only sense the movement at length scales larger than ∼10 nm, and thus any nanoheterogeneities are averaged out. With nuclear spin as the probe, NMR is generally considered to have greater sensitivity than DRS and DMA. However, modern DRS has the advantage of very wide frequency and temperature windows and therefore is frequently used to explore molecular mobility in multicomponent polymer systems.[2] For miscible binary polymer blends with weak intermolecular interactions and a T_g difference between the components (ΔT_g) of ≤50 K, thermorheological simplicity is usually expected.[3] In contrast, complicated relaxation dynamics are observed for blends with large ΔT_g, as demonstrated in studies of polyisoprene/poly(vinylethylene) (PI/PVE, $\Delta T_g \approx 60$ K),[4] polystyrene/poly(vinyl methyl ether) (PS/PVME, $\Delta T_g \approx 130$ K),[5,6] and poly(2-chlorostyrene) (P2CS)/PVME ($\Delta T_g \approx 154$ K).[7] For example, in a 50/50 wt % PI/PVE blend, PI behaves dynamically in a fashion similar to neat PI, while the PVE α process is significantly "plasticized".[4] Two separate dielectric α processes have also been observed in P2CS/PVME blends in the one-phase region and were assigned to the relaxation of the component polymers.[7]

At present, the most popular mechanism for explaining the observation of multiple segmental processes in melt-miscible blends is the concentration fluctuations (CF) model, which proposes a dynamic physical picture with a distribution of compositions in different cooperative rearranging regions (CRR). The CF model of Fischer et al. succeeds in reproducing the broadening of an observed single cooperative segmental relaxation (CSR) but cannot explain the observation of two microenvironments with distinctively different average mobilities and the two separate CSRs in miscible polymer blends.[8] Kumar and Colby et al.[9,10] proposed that the size of the CRR is dependent on the local composition. Satisfactory agreement is obtained when comparing their model with NMR and dielectric data on PI/PVE.

The recent model of Lodge and McLeish[11] proposes that the local environment of a monomer unit in a miscible polymer blend must be rich in species of the same type due to chain connectivity, and the effective local composition is equal to $\Phi_s + (1 - \Phi_s)\Phi$, where Φ_s is the "self-concentration" and Φ the bulk composition. The Φ_s for the low-T_g component is generally larger because it is more flexible, and the local dynamics in the blended environment may be quite similar to that of the neat component.

Chung et al. have argued that the large difference between the fast and slow segmental relaxation rates in PI/PVE blends observed in their 2D NMR experiments cannot be explained by a simple CF model and that intrinsic mobility differences between the two species needs to be considered.[12] The mobility difference between the components in PI/PVE blends was found to be nearly an order of magnitude at temperatures far above the global T_g, and the difference is in quantitative agreement with measurements on each component individually.[13] This explanation is similar to one proposed recently by Sy and Mijovic, who invoked the interplay between the physical dimensions of various nanoscopic regions and the different CRR length scales as well as the temperature dependences of the CRR of the individual components.[14]

* To whom correspondence should be addressed: e-mail runt@matse.psu.edu; phone 1-814-8632749; fax 1-814-8650016.

10.1021/ma034874s CCC: $25.00
Published on Web 09/25/2003

To develop an understanding of the glass transition, we have been investigating the relaxation behavior of polymer systems that exhibit strong intermolecular interactions. Hydrogen bonding is generally found to suppress concentration fluctuations and couple the segmental motions in polymer blends. Only one CSR involving both species was observed in DRS experiments on melt-miscible blends of poly(4-vinylphenol) (PVPh) with poly(ethyl methacrylate),[15] poly(vinyl acetate) at 10−40 wt % PVPh,[16] and poly(vinyl ethyl ether) (PVEE) at 30−50 wt % PVPh.[17] The single segmental relaxation is in accordance with homogeneity on the length scale of 2−3 nm, as suggested by a single composition-dependent ^{1}H $T_{1\rho}$ (proton spin−lattice relaxation time in the rotating frame) in similar blends exhibiting intermolecular hydrogen bonding.[18−21]

The present paper represents an extension of our previous studies of model poly(ethylene oxide) [PEO] blends exhibiting intermolecular hydrogen bonding. The earlier investigations focused primarily on crystallization and microstructure formation (e.g., refs 22 and 23), with only indirect attention paid to the remaining amorphous phase. This first paper in a series of two concentrates on the segmental dynamics of melt-miscible blends of PEO and a random poly(styrene-*co*-*p*-hydroxystyrene) (SHS) copolymer, in the composition range where the blends are amorphous. Infrared spectroscopic analysis of blends of PEO with PVPh[24] and a 55/45 styrene-*co*-hydroxystyrene random copolymer[25] clearly demonstrate the presence of intermolecular hydrogen bonds in these systems. A forthcoming paper will concentrate on the even more complex dynamics of semicrystalline PEO/SHS blends.

2. Experimental Section

2.1. Materials. The PEO was purchased from Polysciences. M_w and M_n were determined to be 2.2×10^5 and 5.4×10^4, respectively, as determined from gel permeation chromatography (GPC), using dimethylformamide containing 0.05 M LiBr as the mobile phase. Calibration was performed using PEO standards ($M_w/M_n < 1.1$) from Polymer Standards Service. The SHS copolymer was obtained from Hoechst Celanese and has $M_w = 9.95 \times 10^4$ (polystyrene-equivalent value from GPC**)** and PDI = 2.8. It is composed of 50 wt % styrene and *p*-hydroxystyrene. The styrene concentration was determined by Fourier transform infrared (FTIR) spectroscopy, using an empirical relationship between styrene content measured from NMR and the FTIR absorbance of the 1492 and 1512 cm^{-1} bands.[26] All FTIR spectral absorbance fell within the range of Beer's law. Blends are identified in the text as S*w*, where *w* is the weight percentage of SHS in the mixture.

DRS samples of neat SHS and PEO samples were pressed at 170C and 100 °C, respectively, for several minutes, and then placed into a vacuum oven preheated at 160 and 100 °C, respectively. After heating in a vacuum for 45 min, the heater was turned off, and the samples were kept under vacuum for a day until the oven slowly cooled to room temperature. SHS/PEO blends were prepared from solutions in 50/50 wt % $CHCl_3$/THF. Mixed solutions were stirred for about 6 h. After solution-casting onto Al foil, samples were placed in a hood for ∼12 h and then heated in a vacuum with the temperature gradually increased to avoid bubble formation. The final temperatures were 100, 110, and 120 °C for the S60−S70, S80, and S90 blends, respectively. The temperatures were selected to be higher than T_g values estimated from the Fox equation. After heating at the final temperature for 45 min, the heater was turned off, and samples were maintained under vacuum until the oven slowly cooled to room temperature.

2.2. Techniques. a. DSC. All DSC measurements were performed on a TA Instruments Q-100 apparatus. The temperature and transition enthalpy were calibrated with an indium standard. Heating and cooling rates were 10 °C/min. Sample weights were ∼10 mg.

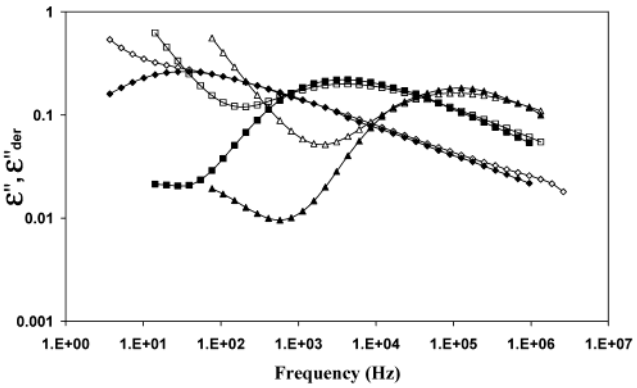

Figure 1. Comparison of the measured dielectric loss, ϵ'' (open symbols), and calculated "conduction-free" dielectric loss, ϵ''_{der} (closed symbols), for the neat SHS copolymer at 160 °C (diamonds), 175 °C (squares), and 190 °C (triangles).

b. FTIR Spectroscopy. 2% solutions of the neat polymers and blends in 50/50 wt % THF/$CHCl_3$ were cast onto KBr windows. After most solvent had evaporated at room temperature, the windows were heated under vacuum at 90 °C for >12 h. FTIR spectra were obtained using a Bio-Rad FTS-6 spectrometer with a resolution of 2 cm^{-1}. Signals of 64 scans were averaged.

c. Dielectric Relaxation Spectroscopy. DRS spectra were collected using a Novocontrol Concept 40 broadband dielectric spectrometer. Temperature control was accomplished using a Novocontrol Quatro Cryosystem. Experiments were run in the frequency domain [0.01 Hz−10 MHz], using 2.5, 5, or 7.5 °C increments. The minimum stabilization time at a given temperature was 1 min. Samples were cooled and heated in the presence of N_2 during the measurements. Dielectric specimens were 0.2−0.5 mm thick and had diameters a little larger than that of the upper electrode (20 mm). Samples were sandwiched between two electrodes and tested between −140 and 200 °C (±0.1 °C stability).

DRS Data Processing. A derivative method was used to aid in analyzing the DRS data. Steeman and van Turnhout reported that the first derivative of the real part of the dielectric constant (ϵ') provides an "ohmic conduction-free" dielectric loss, ϵ''_{der}:[27]

$$\epsilon''_{der} = -\frac{\pi}{2}\frac{\partial \epsilon'(f)}{\partial \ln f} \tag{1}$$

To perform the differentiation, we used a numerical technique based on a low pass quadratic least-squares filter.[28] Figure 1 shows a comparison of the measured loss and calculated ϵ''_{der} for neat SHS at three different temperatures. In a series of model calculations, ϵ''_{der} and ϵ'' have been shown to exhibit the same peak frequencies, and as long as the relaxations are relatively broad (as they are in our case), the relaxation strength of a derivative spectrum is a very good approximation to that of ϵ''.[29] Relaxation peak temperatures (T_{max}) at different frequencies were read from the contour plot of ϵ''_{der}.

3. Results and Discussion

3.1. DSC. Blends containing more than 50% SHS are amorphous and exhibit single glass transitions temperatures (Figure 2). The widths of the glass transitions ($W(T_g)$) for the blends are broader than those of neat SHS, indicating a more heterogeneous relaxation environment. With increasing SHS%, the glass transition interval becomes narrower, and the origin of this will be discussed together with the DRS data.

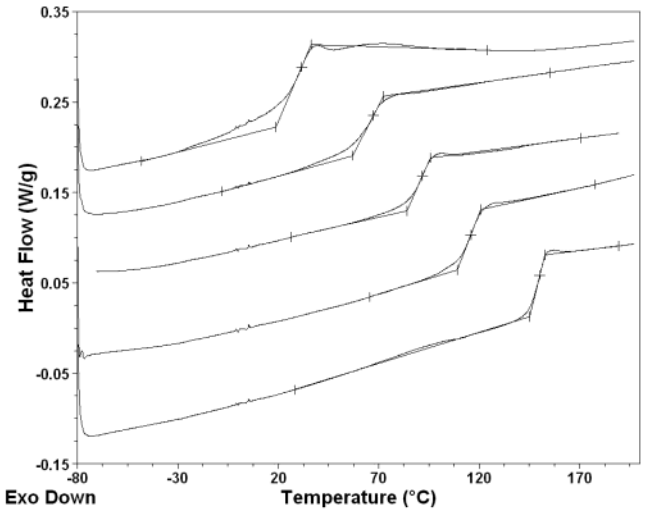

Figure 2. DSC thermograms of amorphous blends containing (from top to bottom in the figure) 60, 70, 80, 90, and 100 wt % SHS.

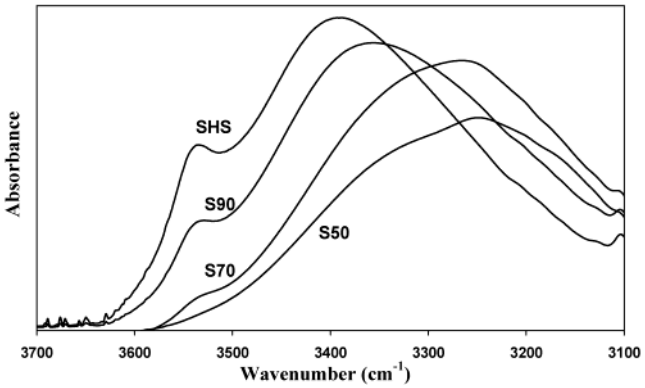

Figure 3. FTIR spectra at room temperature for SHS and selected PEO/SHS blends.

3.2. FTIR. The absorbances in the FTIR spectra of SHS and the blends (Figure 3) can be assigned confidently with reference to the previous extensive FTIR studies on PVPh blends.[24] In the spectrum of neat SHS, "free" and intramolecularly self-associated −OH produce absorbance bands at 3540 and 3390 cm^{-1}, respectively. Intermolecular hydrogen bonds between the phenolic −OH and ether oxygen atoms in PVPh/polyether blends (located near 3250 cm^{-1} in the spectra in Figure 3) have been demonstrated to be stronger than the −OH self-associations in PVPh.[24] Similar conclusions can be drawn from the spectra in Figure 3. The shape and location of the absorbance associated with hydrogen-bonded −OH reflect the increasing ratio of inter- to intramolecular hydrogen bonds with increasing PEO content in the blends. Note that unassociated phenolic −OH's appear in spectra beginning at 70% SHS content.

3.3. DRS. 3.3.1. SHS Copolymer. The DRS spectra of neat SHS (Figure 4) display a CSR process (which we term α_S) and two sub-T_g transitions (β_{S1}, β_{S2}) having apparent activation energies (E_a) of 55 and 33 kJ/mol, respectively. The relaxation dynamics of polystyrene and its derivatives have been studied extensively.[30] Only a dielectric α relaxation is observed for PS: a low-temperature β process is only observed after introducing a polar group on the phenyl ring. The dielectric relaxation strength ($\Delta\epsilon$) of the α process of neat polystyrene was reported to be 0.019[31] and has a weak temperature dependence. Consequently, the β process of PS is

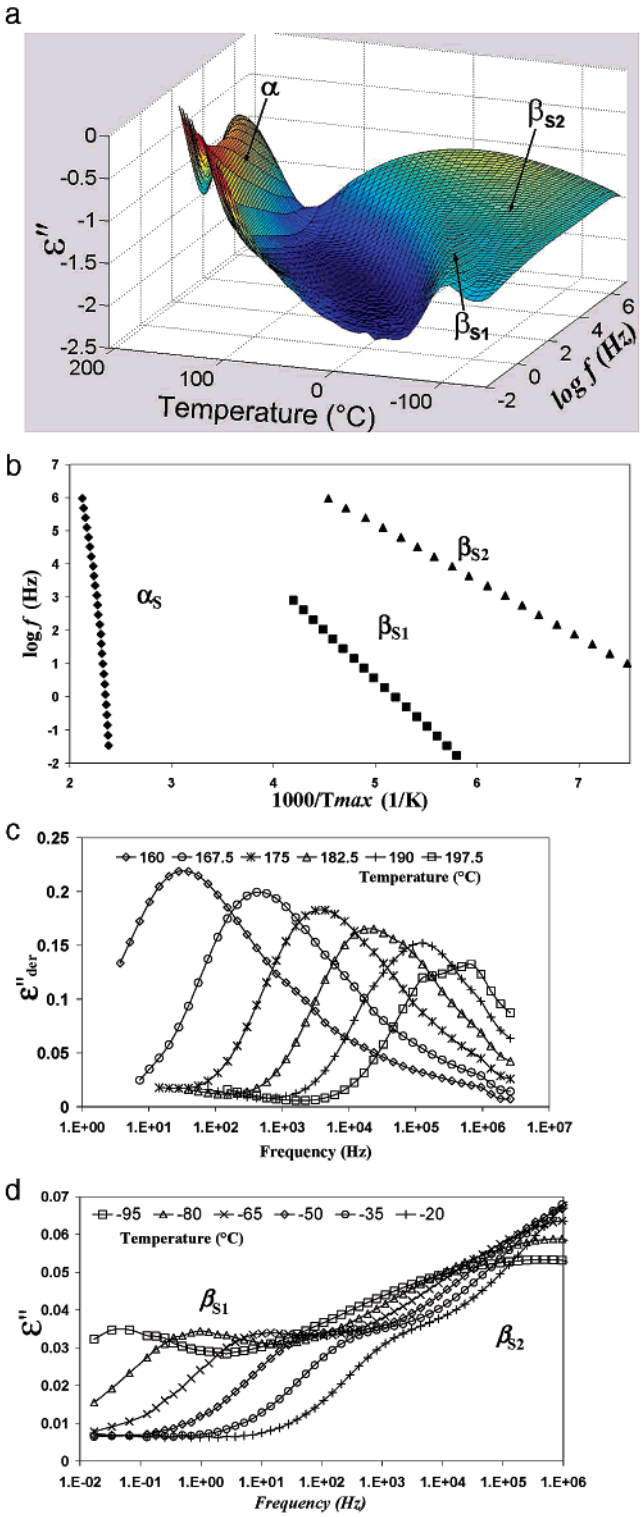

Figure 4. Dielectric relaxation behavior of neat SHS: (a) 3D dielectric ϵ''_{der} spectrum; (b) Arrhenius plot; (c) high-temperature frequency plane spectra of the α relaxation; (d) low-temperature frequency plane spectra of the β_{S1} and β_{S2} processes.

expected to be even weaker. Therefore, the β_{S1} and β_{S2} relaxations are related to the hydroxystyrene repeat units.

Generally, because of the enhanced thermal energy with increasing temperature, $\Delta\epsilon$ of a cooperative segmental relaxation decreases due to decreased cooperativity, and that of a noncooperative local relaxation increases because of increased dipole fluctuation angle

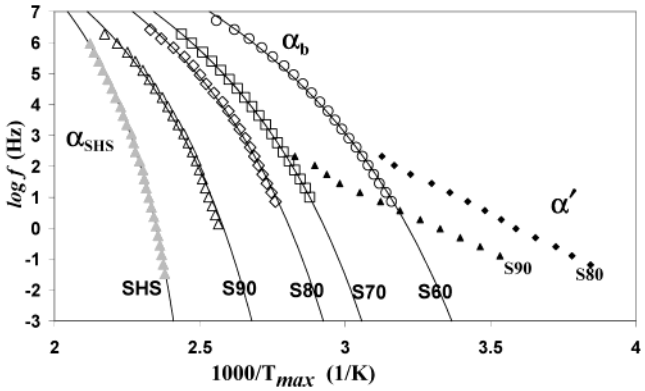

Figure 5. Arrhenius plot for blends with 60−100 wt % SHS: gray triangles, SHS. Open symbols: circles, S60; squares, S70; diamonds, S80; triangles, S90. The solid lines through the data for the α processes are the fits of the VFT expression. Filled symbols are the data for the α′ process for S80 and S90.

Table 1. VFT Fitting Parameters and Fragilities for SHS and the Blends

	S60	S70	S80	S90	SHS
B (K)	2260	2320	2290	2320	1710
T_0 (°C)	−37	−8	7	38	96
T(100 s) (°C)	25	55	70	101	143
m (100 s)	78	84	88	95	142
T_g (onset)	20	57	84	109	145

and the fraction of mobile groups.[32] Thus, the change in $\Delta\epsilon$ with temperature can be a useful tool for indicating the extent of cooperativity of a particular relaxation. The fact that $\Delta\epsilon(\beta_{S1})$ is almost insensitive to temperature (Figure 4d) suggests that the β_{S1} process is more cooperative than typical local processes.

Although we have investigated the influence of hydrogen bonding on dynamics of some neat polymers and blends, especially PVPh and its copolymers,[16,17] these studies concentrated primarily on the segmental processes. de la Rosa et al. have recently undertaken studies on the secondary relaxations of poly(vinyl alcohol), poly(allyl alcohol) (PAA), and polysaccharides using both experiments and modeling.[33] They observed a slightly cooperative secondary relaxation, as well as a noncooperative one, for PAA and polysaccharides. Considering the simple chemical structure of PAA, the slight cooperativity is likely associated with hydroxyl groups that participate in hydrogen bonds with neighboring units. Analogously, we associate the β_{S1} and β_{S2} processes in SHS with hydroxystyrene units that are hydrogen-bonded (self-associated in neat SHS) and unassociated, respectively. Both species are shown to be present in significant amounts in FTIR spectra.

3.3.2. Segmental α Process. a. VFT Fitting and Time−Temperature Superposition (TTS). As noted earlier, for certain compositions of PVPh/PVEE blends, intermolecular hydrogen bonding was found to be capable of coupling the CSRs of the component polymers, having much different T_g's. Large T_g contrast and hydrogen bonding also characterize the SHS/PEO system, and PEO and PVEE have some similarities in repeat unit structure. In fact, it is plausible that hydrogen bonding is the principal factor determining the segmental relaxation of SHS/PEO blends. Figure 5 displays the relaxation frequencies/temperatures of the segmental process of SHS, the α_b process of the blends, and the fit of the data sets with the Vogel−Fulcher−Tammann (VFT) expression:

$$f = f_0 e^{-B/(T-T_0)} \tag{2}$$

where f_0, B, and T_0 are fitting parameters. T_0 is sometimes referred to as the ideal T_g or Vogel temperature and is related to zero fraction of free volume[34] or diverged volume of the cooperative rearranging region.[35]

From the equivalence of the WLF and VFT equations, Angell[36] deduced that

$$C_1(T_g) = \log\left(\frac{\tau(T_g)}{\tau_0}\right) \tag{3}$$

where C_1 is a constant in the WLF equation (∼16 for most polymers, when T_g is taken as the reference temperature). Angell[37] reported that the temperature at which the relaxation time for the fundamental enthalpic relaxation process reaches 100 s is close to the T_g obtained from standard scanning measurement, specifically the temperature at which the heat capacity jump characteristic of the glass transition commences at heating rate of 10 °C/min. Thus, when fixing C_1 as 16 and $\tau(T_g)$ as 100 s, one obtains $\tau_0 \sim 10^{-14}$ s, the phonon-like value. This τ_0 ($f_0 = {}^1/_{2\pi\tau_0}$) was used in our VFT fitting. T_{ref}(100 s) (i.e., the temperature at which τ reaches 100 s) derived from our VFT fitting of the DRS data (Table 1) is in fact near the DSC onset T_g. In addition, the difference between T_0 and T(100 s) is about 60 and 50 °C for the blends and neat SHS, respectively, which is in agreement with the usual expectations.

The loss data (α_b for blend and α_s for neat SHS) at different temperatures can be shifted to form a normalized master curve; i.e., the TTS principle is valid for SHS and the blends. Data for the S70 blend and SHS are provided as examples in Figure 6. The normalized data at different compositions are compared at 45 °C + T(100 s) in Figure 6c. The width of the segmental relaxation gradually narrows with increasing SHS content, in agreement with the findings of the DSC experiments.

b. Fragility. Fragility is a measure of the rapidity with which a material changes its mean relaxation time in the vicinity of T_g, and it is used extensively to classify glass formers.[38] The dynamic fragility, m, is widely used and is defined

$$m = \frac{\mathrm{d}\log\tau_{max}}{\mathrm{d}(T_{ref}/T)}\Big|T=T_{ref} \tag{4}$$

where T_{ref} is a reference temperature, which normally takes a value close to T_g. Replacing f with $1/(2\pi\tau)$ and taking the first derivative of the VFT expression, one obtains

$$m = \frac{B}{T_{ref}(\ln 10)\left(1 - \frac{T_0}{T_{ref}}\right)^2} \tag{5}$$

The VFT fit parameters and calculated values of the dynamic fragility m are listed in Table 1.

There have only been a modest number of reports concerning the effect of hydrogen bonding on polymer fragilities. Fragilities for random copolymers of styrene and hydroxystyrene have been reported to be independent of copolymer composition up to 18 mol % hydroxystyrene.[31] The fragility calculated from our experimental data for the SHS copolymer (142) is therefore reasonable in comparison to that determined for PS with compa-

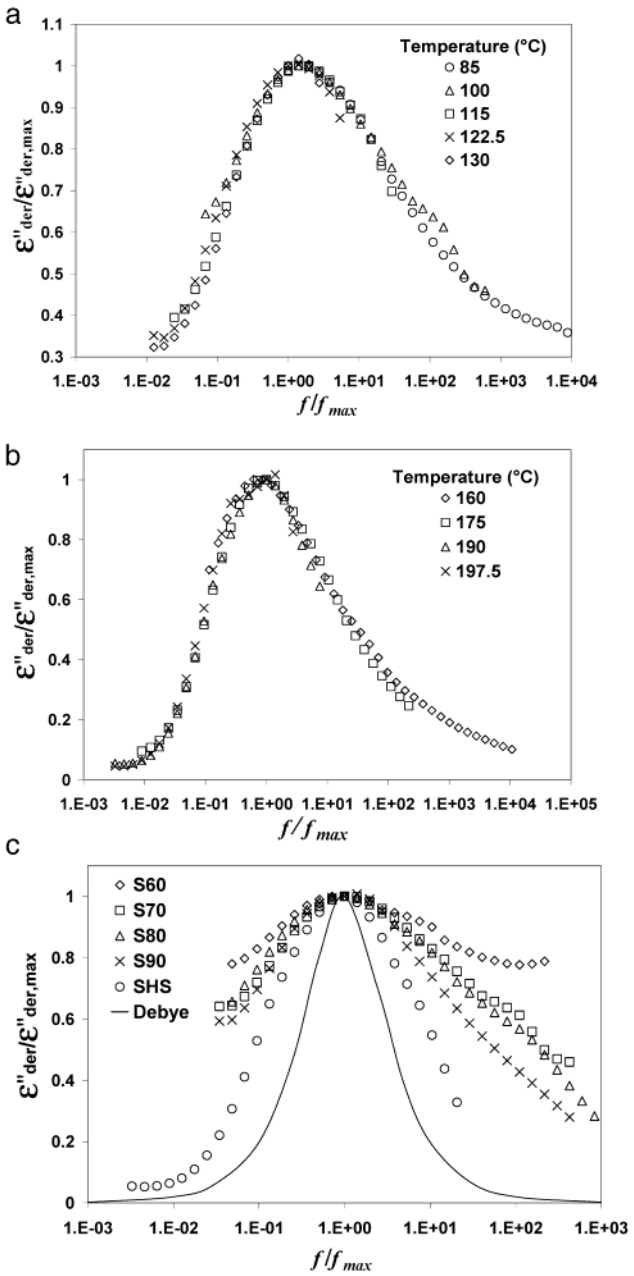

Figure 6. Master curves for the α process of (a) S70 and (b) neat SHS. (c) Normalized loss curves for the various blends and SHS at T_g + 45 °C.

rable M_w (140).[39] The blend fragility increases rather significantly with increasing SHS content (Table 1), in accordance with previous results on PVPh blends with poly(methyl acrylate),[40] poly(vinyl ethyl ether),[17] poly(vinyl acetate), and poly(ethylene-*co*-vinyl acetate).[16]

It has been concluded previously that the backbones of strong glass formers are smooth, compact, symmetric, and flexible, and polymers with less flexible backbones and/or sterically hindering groups exhibit high fragility.[41] PEO and SHS fit these criteria of strong and fragile glass formers, respectively. The blend fragility should, of course, reflect the characteristics of the blend segments. Santangelo et al. proposed that the relaxation of a segment depends on the constraints of the neighboring segments.[42] This idea was used later to explain the fragilities of various homopolymers, and free volume considerations were proposed to be unnecessary.[43] Typical values of the length scale of cooperativity for

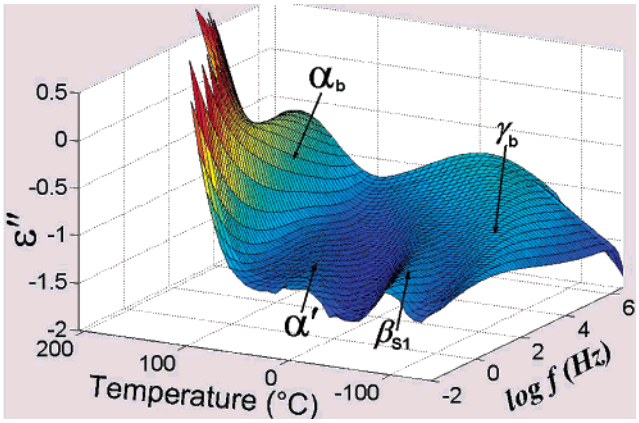

Figure 7. 3D dielectric ϵ''_{der} spectra for the S90 blend. The β_{S1} and γ_b processes at low temperatures are local relaxations, which will be discussed in our next paper.

polymers at T_g are ∼3 nm.[44] Therefore, in a binary polymer blend, during the cooperative segmental process, the coupled bond rotations within several connected repeat units of one polymer chain must be affected by the surrounding units, which are not necessarily from the same chain or even the same component, particularly when there is intermolecular hydrogen bonding. This idea is supported by previous reports that amorphous PVPh/PEO mixtures are homogeneous on a scale of 2−3 nm at 310 K,[45] and the molecular motions of PVPh and PEO affect each other strongly.[46] Therefore, with increasing SHS content, both components combine to establish the characteristics of the segmental relaxation, resulting in a fragility closer to that of neat SHS at higher SHS blend compositions.

3.3.3. The α′ Process. For the 80% and 90% SHS blends a process emerges between the sub-glass and α_b relaxations, which we term the α′ process (see Figures 5 and 7). Its relaxation frequency/temperature behavior is Arrhenius-like (see Figure 5) with an activation energy for S80 and S90 of ∼90 kJ/mol, somewhat higher than typical E_a of general secondary relaxations (20−50 kJ/mol[32]). The relaxation strength of the α′ process clearly decreases with increasing temperature for the S80 blend (Figure 8a) but becomes almost insensitive to temperature for S90 (Figure 8b), suggesting reduced cooperativity on going from the S80 to S90 blend. Although the α′ relaxation has an activation energy only a bit higher than a typical secondary process, unlike a local process, it shifts to higher temperatures with increasing SHS content, like the α_b relaxation. We have recently observed the same unique relaxation behavior in other globally miscible blends, e.g., in SHS/PVEE[47] and PVPh/PVME[48] blends, at high concentrations of SHS and PVPh, respectively.

It may at first be expected that the concentrations of relaxing species in blends with strong intermolecular interactions are unimodal and distributed rather narrowly around the mean composition. However, the number of hydrogen bonds is strongly affected by chain connectivity and the spacing of functional groups, which effectively reduces the intermolecular hydrogen bonding contribution to the free energy of mixing.[49] The local SHS self-concentration can be enhanced further by intramolecular hydrogen bonding between −OH groups. With the parameters in Table 2[50] and using the procedure described in ref 51, we estimate that in the S90 blend at 60 °C about 29% of SHS −OH groups are *inter*molecularly hydrogen bonded, while ∼52% are

Table 2. Parameters Used To Calculate Intermolecular Hydrogen Bond Fractions

	molar vol (cm^3/mol)	solubility parameter $(cal/cm^{-3})^{0.5}$	structural unit mol wt (g/mol)	equilib constants of H bond formation at 25 °C[d]		
				K_2	K_B	K_A
SHS[b]	208	10.2	240	9.4	29.8	39.3
PEO[c]	38.1	9.4	44.1			

[a] Intramolecular screening factor was set to 0.3 in all calculations. [b] For calculation of molar volume and unit molecular weight, the SHS structural unit was considered to contain one hydroxystyrene unit and the appropriate number of styrene units based on copolymer composition. The molar volume and solubility parameter of SHS were obtained using the volume average of those of polystyrene and PVPh. The PVPh data used were those in ref 50, and the PS data were calculated in the same manner as PEO (see note *c*). [c] The PEO molar volume and solubility parameter were calculated using the group contribution method and the data from the Penn State Data Bank. [d] K_2 is the equilibrium constant for intramolecular dimer formation, K_B that for intramolecular multimer formation, and K_A that for the intermolecular hydrogen bond between PEO and SHS. The corresponding enthalpies of hydrogen bond formation are $h_2 = -5.60$, $h_B = -5.20$, and $h_A = -5.4$ kcal/mol.

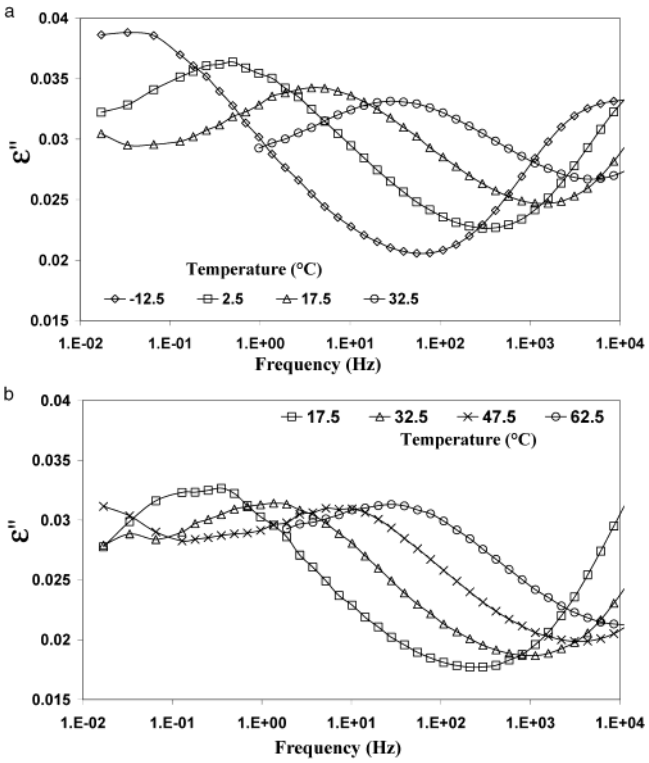

Figure 8. Frequency plane dielectric loss spectra of the α′ relaxation in (a) S80 and (b) S90. Solid lines are only to guide the eye.

*intra*molecularly hydrogen bonded. In addition, repulsion between styrene units in SHS and PEO segments is expected, considering the large-scale phase separation observed in blends of PS and PEO.[52] All of these factors contribute to a broadened distribution of segmental relaxation times in these blends.

In light of the very different intrinsic mobilities of the two components, as reflected by their large T_g difference (∼206 °C), and with reference to the different characteristic temperature dependences of PVPh and PEO in blends as observed in NMR experiments,[46] we propose that PEO-rich local environments relax at temperatures below the global blend T_g, i.e., give rise to the α′ process. SHS segments in the vicinity of relaxing PEO segments are unlikely to be able to follow the relaxation since the number of the latter is too low to modify the rigid local SHS environment until the blend T_g is reached. The sequence length of PEO repeat units participating in the α′ process is limited since some are hydrogen bonded to hydroxystyrene repeats. On the basis of the FTIR spectrum and the procedure described above, we estimate that about 48% of PEO ether groups are hydrogen bonded in the S90 blend at 60 °C. There will be a sequence length distribution for the remaining unassociated repeat units, but the overall length scale will be small, perhaps roughly on the order of 1 nm. On the basis of the view that the typical size of a cooperative rearranging region is ∼3 nm at T_g,[44] these unassociated PEO units can only relax in a noncooperative way. In addition, the participating PEO repeat units are under confinement by neighboring SHS segments that are still frozen at this relatively low temperature. As SHS content increases, there is a greater probability for hydrogen bonding to the PEO −O−, decreasing the probability of organizing a sufficient number of unassociated PEO repeat units in order to observe an α′ relaxation, until the hydrogen-bonded fraction decreases sufficiently at higher temperatures. This is in keeping with the shift of the α′ process to higher temperatures in the 90% SHS blend, together with the α_b relaxation.

The most prominent feature of the α′ process is the reduced cooperativity, as deduced from the activation energy and temperature dependence of the relaxation strength. The behavior of the α′ process is reminiscent of recent findings of polymer dynamics in polymer nanocomposites and ultrathin polymer films. For example, it has been reported that for a 1.5−2.0 nm layer of poly(methylphenylsiloxane) (PMPS) sandwiched between parallel silicate layers, the normal PMPS segmental relaxation is replaced by a faster process with reduced cooperativity.[53] It has been proposed that two effects can reduce the cooperativity of the segmental relaxation in ultrathin polymer layers.[54] One is chain orientation induced parallel to the surface when layer thickness is smaller than the end-to-end distance of the polymer chains. The other is a finite-size effect: if the scale of the confinement is smaller than the CRR, normal cooperative segmental relaxations will be limited and a modified fast process emerges, which probably involves fewer repeat units and is less cooperative than normal segmental processes.

4. Summary

The calculated fragility of the 50/50 SHS copolymer was found to be near that of unmodified polystyrene, suggesting that intramolecular hydrogen bonding has little effect on fragility. Two local relaxations are observed in SHS at low temperatures and assigned to unassociated and hydrogen-bonded hydroxystyrene units, respectively.

Despite the large T_g difference between PEO and SHS, a single dominant segmental relaxation is observed for blends with SHS concentration ≥60%, demonstrating the coupling ability of intermolecular hydrogen bonds. The dielectric CSR processes of all of the amorphous blends are fit well by the VFT equation, and the temperature at which the relaxation time reaches

100 s is close to the onset of the heat capacity increase at T_g. In agreement with our previous results on other blends exhibiting intermolecular hydrogen bonding, blend fragility gradually increases with increasing SHS content.

Finally, we also observed an additional fast process in blends containing 80 and 90 wt % SHS. The evidence supports its assignment to noncooperative segmental relaxation of PEO repeat units. This process has some similarities (i.e., noncooperativity and rigid local environment) to the modified segmental relaxation observed for polymers in ultrathin films and layered silicate nanocomposites.

Acknowledgment. We express our appreciation to the National Science Foundation, Polymers Program (DMR-0211056), for its support of this research and the NSF-MRI program for support of the dielectric instrumentation (DMR-0079432).

References and Notes

(1) (a) Quan, X.; Johnson, G. E.; Anderson, E. W.; Bates, F. S. *Macromolecules* **1989**, *22*, 2451. (b) Miller, J. B.; McGrath, K. J.; Roland, C. M.; Trask, C. A.; Garroway, A. N. *Macromolecules* **1990**, *23*, 4543. (c) Schmidt-Rohr, K.; Clauss, J.; Spiess, H. W. *Macromolecules* **1992**, *25*, 3273.
(2) Runt, J., Fitzgerald, J. J., Eds. *Dielectric Spectroscopy of Polymer Materials: Fundamentals and Applications*; American Chemical Society: Washington, DC, 1997.
(3) (a) Pathak, J. A.; Colby, R. H.; Kamath, S. Y.; Kumar, S. K.; Stadler, R. *Macromolecules* **1998**, *31*, 8988. (b) Alegria, A.; Elizetxea, C.; Cendoya, I.; Colmenero, J. *Macromolecules* **1995**, *28*, 8819.
(4) Arbe, A.; Alegria, A.; Colmenero, J.; Hoffmann, S.; Willner, L.; Richter, D. *Macromolecules* **1999**, *32*, 7572.
(5) Pathak, J. A.; Colby, R. H.; Floudas, G. Jérôme, R. *Macromolecules* **1999**, *32*, 2553.
(6) (a) Cendoya, I.; Alegria, A.; Colmenero, J.; Grimm, H.; Richter, D.; Frick, B. *Macromolecules* **1999**, *32*, 4065. (b) Roland, C. M.; Ngai, K. L. *Macromolecules* **1992**, *25*, 363.
(7) Urakawa, O.; Fuse, Y.; Hori, H.; Tran-Cong, Q.; Yano, O. *Polymer* **2001**, *42*, 765.
(8) (a) Katana, G.; Fischer, E. W.; Hack, T.; Abetz, V.; Kremer, F. *Macromolecules* **1995**, *28*, 2714. (b) Zetsche, A.; Fischer, E. W. *Acta Polym.* **1994**, *45*, 168.
(9) Kumar, S. K.; Colby, R. H.; Anastasiadis, S. H.; Fytas, G. *J. Chem. Phys.* **1996**, *105*, 3777.
(10) Kamath, S.; Colby, R. H.; Kumar, S. K.; Karatasos, K.; Floudas, G.; Fytas, G.; Roovers, J. E. L. *J. Chem. Phys.* **1999**, *111*, 6121.
(11) Lodge, T. P.; McLeish, T. C. B. *Macromolecules* **2000**, *33*, 5278.
(12) Chung, G. C.; Kornfield, J. A.; Smith, S. D. *Macromolecules* **1994**, *27*, 964.
(13) Min, B.; Qiu, X.-H.; Ediger, M. D.; Pitsikalis, M.; Hadjichristidis, N. *Macromolecules* **2001**, *34*, 4466.
(14) Sy, J. W.; Mijovic, J. *Macromolecules* **2000**, *33*, 933.
(15) Zhang, S. H.; Jin, X.; Painter, P. C.; Runt, J. *Macromolecules* **2002**, *35*, 3636.
(16) Zhang, S.; Painter, P. C.; Runt, J. *Macromolecules* **2002**, *35*, 8478.
(17) Zhang, S. H.; Painter, P. C.; Runt, J. *Macromolecules* **2002**, *35*, 9403.
(18) Yi, J.; Goh, S. H.; Wee, A. T. S. *Macromolecules* **2001**, *34*, 7411.
(19) Yi, J.; Goh, S. H. *Polymer* **2002**, *43*, 4515.
(20) Wang, J.; Cheung, M. K.; Mi, Y. *Polymer* **2001**, *42*, 2077.
(21) Huang, M. W.; Kuo, S. W.; Wu, H. D.; Chang, F. C.; Fang, S. Y. *Polymer* **2002**, *43*, 2479.
(22) Lisowski, M. S.; Liu, Q.; Cho, J. D.; Runt, J.; Yeh, F.; Hsiao, B. S. *Macromolecules* **2000**, *33*, 4842.
(23) Wu, L.; Lisowski, M. S.; Talibuddin, S.; Runt, J. *Macromolecules* **1999**, *32*, 1576.
(24) Moskala, E. J.; Varnell, D. F.; Coleman, M. M. *Polymer* **1985**, *26*, 228.
(25) Ting, S. P.; Bulkin, B. J.; Pearce, E. M. *J. Polym. Sci., Polym. Chem. Ed.* **1981**, *19*, 1451.
(26) Xu, Y. Ph.D. Dissertation, The Pennsylvania State University, 1991.
(27) Steeman, P. A. M.; van Turnhout, J. *Macromolecules* **1994**, *27*, 5421.
(28) Gory, P. A. *Anal. Chem.* **1990**, *62*, 570.
(29) Wübbenhorst, M.; van Turnhout, J. *J. Non-Cryst. Solids* **2002**, *305*, 40.
(30) McCrum, N. G.; Read, B. E.; Williams, G. *Anelastic and Dielectric Effects in Polymer Solids*; Dover Publications Inc.: New York, 1967; pp 409, 327.
(31) Schroeder, M. J.; Roland, C. M.; Kwei, T. K. *Macromolecules* **1999**, *32*, 6249.
(32) Schönhals, A. In Runt, J., Fitzgerald, J. J., Eds.; *Dielectric Spectroscopy of Polymer Materials: Fundamentals and Applications*; American Chemical Society: Washington, DC, 1997; p 107.
(33) (a) de la Rosa, A.; Heux, L.; Cavaillé J. Y. *Polymer* **2001**, *42*, 5371. (b) de la Rosa, A.; Heux, L.; Cavaillé J. Y.; Mazeau, K. *Polymer* **2001**, *42*, 5665.
(34) Grest, G. S.; Cohen, M. H. *Adv. Chem. Phys.* **1981**, *48*, 455.
(35) Donth, E. *Relaxation and Thermodynamics in Polymers: Glass Transition*; Akademie-Verlag: Berlin, Germany, 1992.
(36) Angell, C. A. *Polymer* **1997**, *38*, 6261.
(37) Angell, C. *A. J. Non-Cryst. Solids* **1991**, *131*−*133*, 13.
(38) Angell, C. A. *Science* **1995**, *267*, 1924.
(39) Santangelo, P. G.; Roland, C. M. *Macromolecules* **1998**, *31*, 4581.
(40) Prolongo, M. G.; Salom, C.; Masegosa, R. M.; Moreno, S.; Rubio, R. G. *Polymer* **1997**, *38*, 5097.
(41) Ngai, K. L.; Roland, C. M. *Macromolecules* **1993**, *26*, 6824.
(42) Santangelo, P. G.; Ngai, K. L.; Roland, C. M. *Macromolecules* **1993**, *26*, 2682.
(43) Roland, C. M.; Ngai, K. L. *J. Non-Cryst. Solids* **1994**, *172*−*174*, 868.
(44) Donth, E. *J. Polym. Sci., Polym. Phys.* **1996**, *34*, 2881.
(45) Zhang, X.; Takegoshi, K.; Hikichi, K. *Macromolecules* **1992**, *25*, 2336.
(46) Zhang, X.; Takegoshi, K.; Hikichi, K. *Macromolecules* **1993**, *26*, 2198.
(47) Zhang, S. H.; Jin, X.; Painter, P. C.; Runt, J. *Macromolecules* **2003**, *36*, 5710.
(48) Zhang, S. H.; Jin, X.; Painter, P. C.; Runt, J. *Polymer*, submitted for publication.
(49) (a) Hu, Y.; Gamble, V.; Painter, P. C.; Coleman, M. M. *Macromolecules* **2002**, *35*, 1289. (b) Painter, P.; Park, Y.; Coleman, M. *J. Appl. Polym. Sci.* **1998**, 1273.
(50) Serman, C. J.; Xu Y.; Painter, P. C.; Coleman, M. M. *Polymer* **1991**, *32*, 516.
(51) Coleman, M. M.; Graf, J. F.; Painter, P. C. *Specific Interactions and the Miscibility of Polymer Blends*; Technomic Publishing: Lancaster, PA, 1991.
(52) Smith, T. W.; Abkowitz, M. A.; Conway, G. C.; Luca, D. J.; Serpico, J. M.; Wnek, G. E. *Macromolecules* **1996**, *29*, 5042.
(53) Anastasiadis S. H.; Karatasos, K.; Vlachos, G.; Manias, E.; Giannelis, E. P. *Phys. Rev. Lett.* **2000**, *84*, 915.
(54) Ngai, K. L. *Philos. Mag.* **2002**, *82*, 291.

MA034874S